Monatshefte für Chemie - Chemical Monthly (2022) 153:31–38
https://doi.org/10.1007/s00706-021-02870-z

ORIGINAL PAPER

Electrochemical sensing of antibiotic drug amoxicillin in the presence of dopamine at simple and selective carbon paste electrode activated with cetyltrimethylammonium bromide surfactant

N. Hareesha[1] · J. G. Manjunatha[1] · P. A. Pushpanjali[1] · N. Prinith Subbaiah[1] · M. M. Charithra[1] · N. Sreeharsha[2,3] · S. M. Basheeruddin Asdaq[4] · Md. Khalid Anwer[5]

Received: 1 October 2021 / Accepted: 2 November 2021 / Published online: 16 November 2021

Abstract

The effective, selective, and electrochemically steady cetyltrimethylammonium bromide drop-casted carbon paste electrode was constructed for the detection of amoxicillin in presence of dopamine through cyclic voltammetry method. The modified and unmodified electrode materials were characterized by various methods like field emission scanning electron microscopy, cyclic voltammetry, and electrochemical impedance spectroscopy with acceptable results. The constructed modified sensor delivers a higher electrocatalytic nature for the oxidation of 0.1 mM amoxicillin in 0.1 M phosphate buffer saline of 6.5 pH with high peak current and lower peak potential than the bare carbon paste electrode. The analytical applicability of modified electrode for amoxicillin electro-oxidation was detected by increasing the amoxicillin concentration in the range from 10 to 150 µM with fine limit of detection and the limit of quantification of 5.90 µM and 19.67 µM, respectively. This article discloses a facile and recommended approach for the concurrent inspection of amoxicillin in the presence of dopamine. The modified sensor gives high stability, repeatability, reproducibility, and sensitivity. The premeditated method and modified sensor give a fine recovery for amoxicillin detection in medication sample.

Graphical abstract

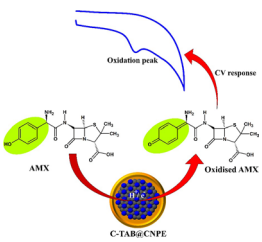

Keywords Amoxicillin · Carbon paste electrode · Surfactant modification · Electrochemical impedance spectroscopy · Voltammetry · Electron transfer · Sensors · Dopamine

✉ J. G. Manjunatha
manju1853@gmail.com

[1] Department of Chemistry, FMKMC College, Constituent College of Mangalore University, Madikeri, Karnataka, India

[2] Department of Pharmaceutical Sciences, College of Clinical Pharmacy, King Faisal University, Al Hofuf 31982, Al-Ahsa, Saudi Arabia

[3] Department of Pharmaceutics, Vidya Siri College of Pharmacy, Off Sarjapura Road, Bengaluru, Karnataka 560 035, India

[4] Department of Pharmacy Practice, College of Pharmacy, AlMaarefa University, Riyadh, Saudi Arabia

[5] Department of Pharmaceutics, College of Pharmacy, Prince Sattam Bin Abdulaziz University, Al-Alkharj 11942, Saudi Arabia

Introduction

Antibiotics (β-lactam group) are the significant antimicrobial mediators that are broadly prescribed to cure infectious disorders in living bodies (human and animal). β-Lactam antibiotics portray a configuration based on a ring called β-lactam which is accountable for antibacterial action and variable side chains. That explicates the key dissimilarities in their pharmacologic and chemical characteristics. Which is typically elected due to its better-absorbed character and oral administration than further β-lactam related antibiotics [1].

Amoxicillin (AMX) is the derivative of 6-aminopenicillanic acid and is the most often used antibiotic for the treatment of many diseases like helicobacter pylori infection, lyme disease-arthritis, endocarditis prophylaxis, erythema chronic migraines, chlamydia infection, pharyngitis, middle ear infection, strep throat, pneumonia, skin infection, dental abscesses, and urinary tract infection. Also, AMX shows some serious side-effects in human health such as fever, nausea, hematuria, red or purple skin rashes with peeling and blistering, vomiting, acute allergic infection, anemia, elevated liver enzymes, and serum sickness, sore throat, burning eyes, and vaginal itching [2, 3]. Due to the overdose of AMX some symptoms may accrue in the human body include, stomach upset and diarrhea. Hence, AMX analysis most significantly needs a highly sensitive and fast detection methodology.

Numerous analytical approaches have been documented for the estimation of AMX, like spectrophotometry [4], capillary electrophoresis [5], liquid chromatography with fluorescence [6], high-performance liquid chromatography [7] and so on. But these methods have various drawbacks, such as difficulty to handle, requirement of a large quantity of organic solvents, gives higher limit of detection (LOD) and limit of quantification (LOQ), and needs more operation time, costly instruments, lengthy procedure and standardization. On the opposite side, electrochemical methods are most optimistic for the analysis of AMX due to low cost, rapid response, high selectivity, sensitivity, reproducibility, repeatability, stability and needs simple handling [8–18]. Also, the electroanalytical approaches are the easy-going and broadly operated tools for the analysis of biologically active molecules, purity of pharmacological samples, medical diagnosis, food quality, water, soil, heavy metals and so on, due to their tall responsiveness, selectivity, low expenditure, and simply manageable laboratory surroundings [19–26].

Up-to-date, reports focused on the development of simple, sensitive, selective, low-cost, and eco-friendly electrode materials and surface-active molecules. Modified electrode materials are equipped by the accumulation of different surface-active materials, such as organic molecules (like dyes, surfactants, amino acids, conductive polymers, etc.), nano-metal oxides, activated carbon materials, etc. on the unmodified electrode exteriors. In current centuries, electrode surfaces are modified by coating surfactant molecules that have broadly expanded their consideration.

For the sensitive and selective voltammetric measurement of electro/bioactive molecules, carbon paste electrodes (CNPEs) have been essentially selected due to their easy modification approach, eminent repeatability, reproducibility, stability, implementation of fixed and fine-resolute voltammograms, high thermal and chemical stability, and low-price [27].

Cetyltrimethylammonium bromide (C-TAB, $[(C_{16}H_{33})\text{-}N(CH_3)_3]Br$) is a cationic quaternary ammonium surfactant molecule and the important surface-active agent which helps to improve the sensing capability of the electrode surface. This primary chained monomer adsorbed easily on the surface of the electrode and develop a steady monolayer with a positive charge. Henceforth, the improvement of the impact of C-TAB layer by combining with AMX molecules by adsorption and electrostatic interaction [28]. Also, C-TAB parades supplementary synergetic interaction with CNPE surface, this consequence enhances superior selectivity and sensitivity for the oxidation of AMX molecules. Due to these improved properties, CNPE and C-TAB moieties are used as key mediators for the electrochemical detection of AMX.

In the present effort, we aimed to analyze electrochemical oxidation of AMX by developing a simple, sensitive, and selective cetyltrimethylammonium bromide drop-coasted carbon paste electrode (C-TAB@CNPE). Also, the study of AMX was carried out using the powerful cyclic voltammetry (CV) approach. The electrode materilas were characterised using field emission scanning electron microscopy (FE-SEM), CV, and electrochemical impedance spectroscopy (EIS) methods. The selectivity of the sensor was tested for AMX in the presence of dopamine (DA). The real sample analysis was done using a medicinal sample at the surface of the prepared sensor.

Result and discussions

FE-SEM study of BCNPE and C-TAB@CNPE

The FE-SEM analysis was used to elucidated the surface morphology of bare carbon paste electrode (BCNPE) and C-TAB@CNPE materials. Inset Fig. 1 indicates the FE-SEM images of unmodified (BCNPE) and modified electrode (C-TAB@CNPE) material surfaces. Figure 1a shows

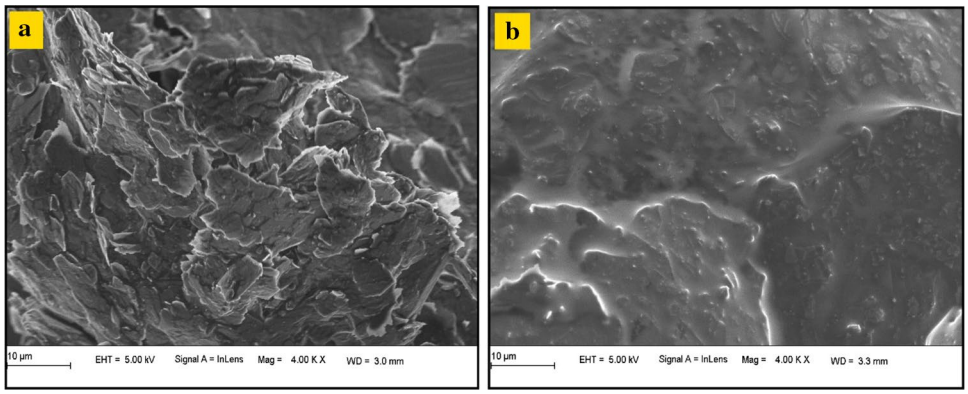

Fig. 1 FE-SEM pictures of **a** BCNPE and **b** C-TAB@CNPE

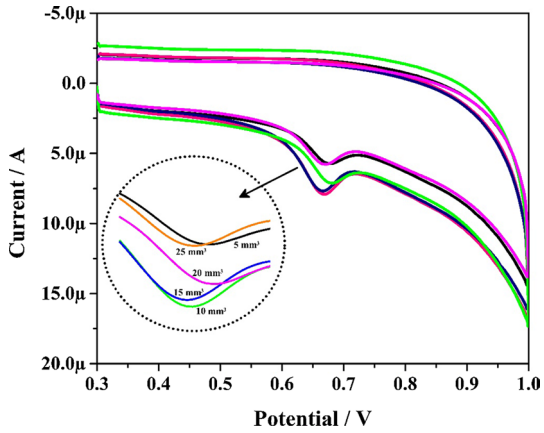

Fig. 2 CVs for 0.1 mM AMX in PBS of 6.5 pH at different concentrations of C-TAB (5.0–25.0 mm^3) on the surface of CNPE

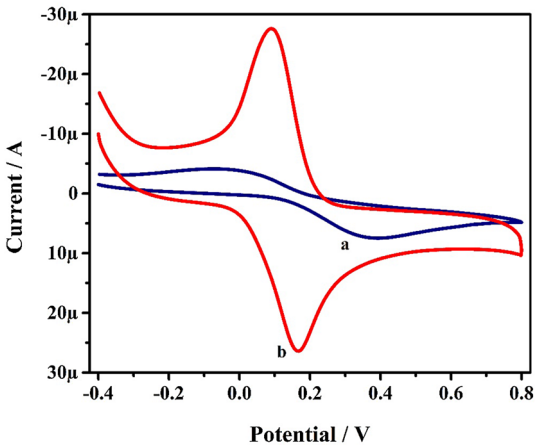

Fig. 3 CVs for 1.0 mM $K_4[Fe(CN)_6]\cdot 3H_2O$ in 0.1 M KCl solution on BCNPE (cycle *a*) and C-TAB@CNPE (cycle *b*) at 0.1 V/s of scan rate and −0.4 to 0.8 V of potential window

the unfinished and asymmetrical shaped flecks with higher cracks which parades the surface morphology of the BCNPE material. Additionally, Fig. 1b shows a thin deposition of C-TAB molecule that are equivalently covered on the external of the CNPE surface which specifies the modified electrode material (C-TAB@CNPE).

Variation of C-TAB concentration

The optimized concentration of C-TAB on the surface BCNTPE was analyzed by varying C-TAB concentration in the range from 5.0 to 25.0 mm^3 for the detection of AMX. Figure 2 denotes the cyclic voltammograms (CVs) for 0.1 mM AMX in phosphate buffer saline (PBS) at different concentrations of C-TAB (5.0–25.0 mm^3) on the surface of CNPE, here the peak current associated to the oxidation of AMX was very high at 10 mm^3 of C-TAB than other C-TAB concentration values (5, 15, 20, and 25 mm^3). This result is most probably due to the effect of the critical aggregation concentration of C-TAB on CNPE surface. Hence, 10 mm^3 of C-TAB was used as optimum concentration for the modification of the surface of CNPE for this experimentation.

Determination of electrochemical surface area

The CV study was adopted for the measurement of the electrochemical active surface area of BCNPE (cycle *a*) and C-TAB@CNPE (cycle *b*) by analyzing the standard analyte 1.0 mM $K_4[Fe(CN)_6]\cdot 3H_2O$ in 0.1 M KCl solution as a supportive buffer at 0.1 V/s of scan rate and −0.4 to 0.8 V of potential window (Fig. 3). The dissimilarity of the redox current of $K_4[Fe(CN)_6]\cdot 3H_2O$ at BCNPE and C-TAB@CNPE is paraded in Fig. 3, here the modified electrode (C-TAB@CNPE) shows less redox peak potential with high redox peak current than BCNPE. This result is because of the reduction of overpotential and more active surface area of the modified electrode. The electrochemical active surface area of the used electrodes was confirmed by the following Randles–Sevcik equation [27],

$$I_p = 2.69 \times 10^5\, n^{3/2} A D^{1/2} C v^{1/2} \quad (1)$$

where I_p is the peak current (A) of $K_4[Fe(CN)_6]\cdot 3H_2O$, n is the number of electrons, A is the electrochemical active surface area (cm^2), D is the diffusion coefficient (cm^2/s), C is the concentration of $K_4[Fe(CN)_6]\cdot 3H_2O$ (M) and υ is the scan rate (V/s). The premeditated electrochemical active surface areas of C-TAB@CNPE and BCNPE were found to be 0.0363 cm^2 and 0.0105 cm^2, respectively. This information discloses that the modified electrode (C-TAB@CNPE) delivers highly sensitive electrochemical platform for the analysis of oxidation nature of AMX than the bare electrode (BCNPE).

EIS study on BCNPE and C-TAB@CNPE

EIS study is the important discipline for assessing the conductive and resistive features of the prepared electrode materials with the interface of the supporting electrolyte. The EIS sequels for BCNPE (cycle *b*) and C-TAB@CNPE (cycle *a*) are elucidated by the appliance of Nyquist diagrams (Fig. 4).

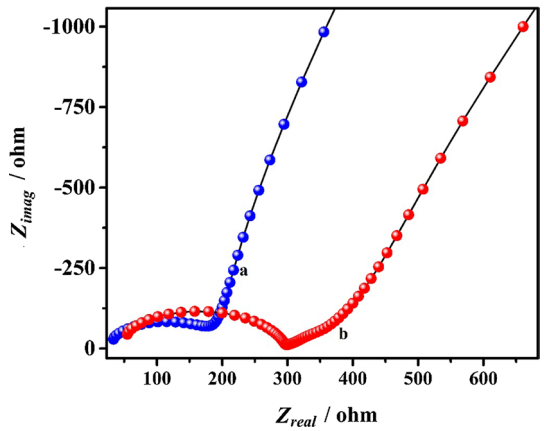

Fig. 4 EIS sequels for BCNPE (cycle *b*) and C-TAB@CNPE (cycle *a*)

The EIS was performed for 1.0 mM $K_4[Fe(CN)_6]\cdot 3H_2O$ in 0.1 M KCl at the operational potential of 0.1 V and amplitude of 0.005 V at the frequency range of 1.0 Hz–1.0 MHz. As of the Nyquist plots (cycle *a* and cycle *b*), the increased semicircle radius of BCNTPE than C-TAB@CNPE detailed that the charge transfer resistance (R_{ct}) is smaller in the modified electrode (C-TAB@CNPE) compared to unmodified electrode (BCNPE) [29].

Study of pH effect on AMX at C-TAB@CNPE

The pH variation was done for the oxidation of AMX at C-TAB@CNPE using CV method is the key aspect for verifying the optimistic pH value with higher peak current. The PBS pH influences the both oxidation peak current and potential of AMX at C-TAB@CNPE. The effect of 0.1 M PBS pH on AMX was verified by changing the PBS pH from 5.5 to 8.0 using the CV method at the scan rate of 0.1 V/s. The CVs (Fig. 5a) for 0.1 mM AMX at C-TAB@CNPE display the shifting of oxidation potential towards the negative side as the increase of PBS pH. The relation pH vs. E_{pa} shows a fine linearity (Fig. 5b) and the linear regression equation is E_{pa} (V) = 1.1782–0.070 pH (V/pH) (R^2 is the correlation coefficient = 0.9964), here the slope (− 0.070 V/pH) is closer to the theoretical value which shows that the oxidation reaction of AMX is continues through the transfer of same number of electrons and protons (1:1 proportion). Additionally, the pH 6.5 gives superior oxidation peak current for AMX, hereafter pH 6.5 was chosen as finest pH for this investigation.

Electrochemical response of AMX at C-TAB@CNPE and BCNPE

The electrochemical response of AMX (0.1 mM) in 0.1 M PBS of pH 6.5 at C-TAB@CNPE and BCNPE was analyzed

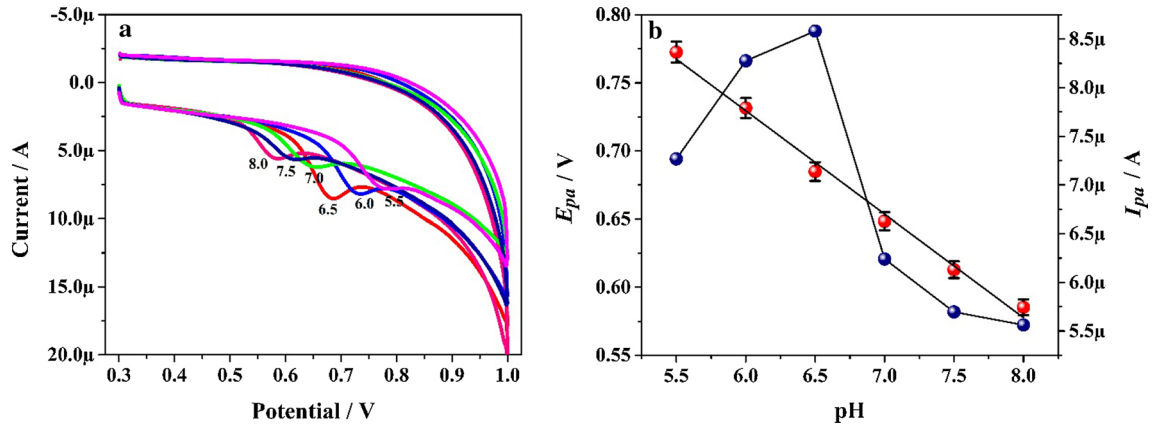

Fig. 5 **a** CVs for 0.1 mM AMX in 0.1 M PBS of different pHs (from 5.5 to 8.0) on C-TAB@CNPE at 0.1 V/s of scan rate. **b** Plots of pH vs. E_{pa} and pH vs. I_{pa}

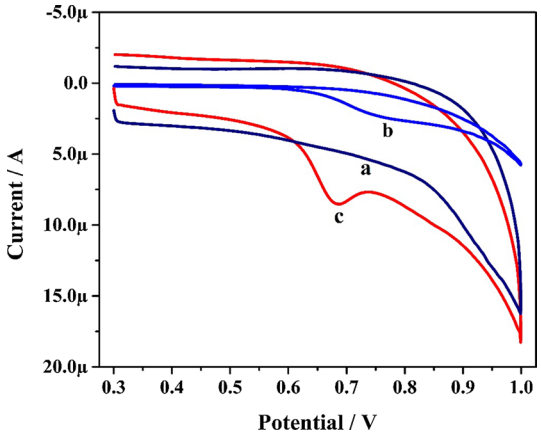

Fig. 6 CVs for the presence and absence (cycle *a*) of AMX (0.1 mM) in 0.1 M PBS of pH 6.5 at C-TAB@CNPE (cycle *c*) and BCNPE (cycle *b*) at the potential gap of 0.3–1.0 V with the scan rate of 0.1 V/s

using CV at the potential domain of 0.3–1.0 V at the scan rate of 0.1 V/s in the presence and absence of AMX. CVs in Fig. 6 discloses that, the absence of AMX (blank, cycle *a*) did not show any electrochemical response. However, the CVs for AMX at BCNPE (cycle *b*) and C-TAB@CNPE (cycle *c*) shows electrochemical response with variable peak current and potentials. Here, BCNPE reveals lower electrochemical action for the oxidation of AMX with lesser peak current response at higher peak potential compare to the modified C-TAB@CNPE. This information defines that C-TAB@CNPE exhibits elevated sensitivity with improved electrocatalytic activity for the oxidation of AMX with fast-rate of electron and proton shift than BCNPE.

Effect of scan rate on the peak potential and current of AMX at C-TAB@CNPE

The effect of scan rate on the oxidation peak response of 0.1 mM AMX in 0.1 M PBS (pH 6.5) at C-TAB@CNPE was inspected by changing the scan rates in the range from 0.05 to 0.25 V/s at the potential gap of 0.3–1.0 V. Figure 7a displays the CVs, where the anodic peak current of each cycle is improved with the slight positive shift in the oxidation peak potentials as the augmentation of each scan rate (0.05–0.25 V/s). Figure 7b indicates the plot of the anodic peak current (I_{pa}) vs. the scan rate (υ) holding a superior linear correspondence and the linear regression equation is $I_{pa}\,(\mu A) = 1.2310 \times 10^{-6} + 3.9804 \times 10^{-5}\,\upsilon\,(V/s)$ ($R = 0.9996$). These data propose that, the catalytic influence of C-TAB@CNPE towards the oxidation of AMX was carry on through the adsorption-controlled kinetics [30]. The electrochemical oxidation of AMX was accomplished by the removal of one electron and one proton from AMX molecule at the surface of C-TAB@CNPE and the probable reaction mechanism is shown in Scheme 1.

Concentration variation of AMX

The electrochemical oxidation of AMX was inspected by varying its concentration in the range from 10.0 to 150.0 µM in 0.1 M PBS of pH 6.5 at C-TAB@CNPE at the scan rate of 0.1 V/s (CVs in Fig. 8a). Figure 8b parades the plot of I_{pa} vs. [AMX], which discloses a fine linear association and the linear regression equation is $I_{pa}\,(A) = 5.9220 \times 10^{-6} + 0.0366$ [AMX] (M) ($R = 0.9980$). The *LOD* and *LOQ* values are premeditated using the following equations $LOD = 3S/M$ and $LOQ = 10S/M$ [31], where S is the standard deviation of blank, and M is the slope of I_{pa} vs. [AMX]. The calculated

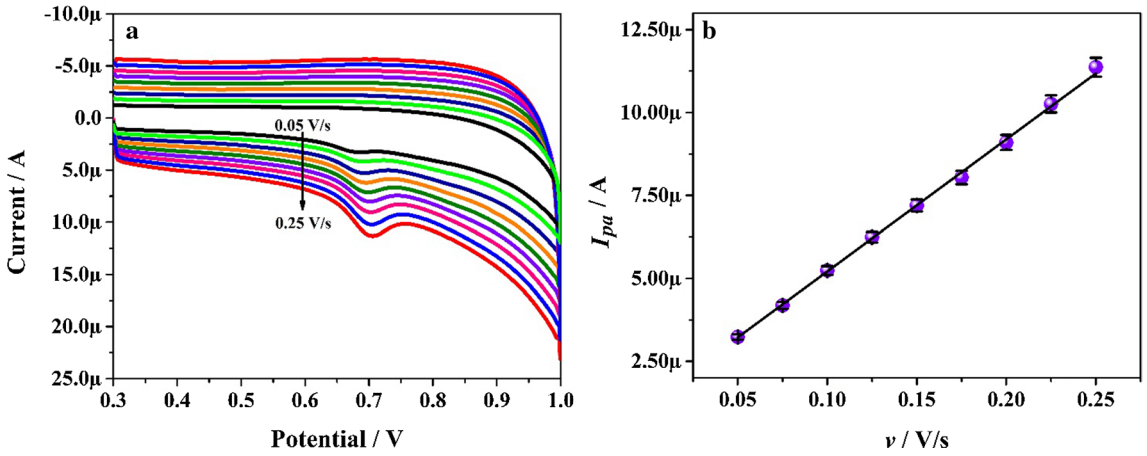

Fig. 7 **a** CVs for 0.1 mM AMX in 0.1 M PBS (pH 6.5) at C-TAB@CNPE at different scan rates in the range from 0.05 to 0.25 V/s at the potential gap of 0.3–1.0 V. **b** Plot of I_{pa} vs. υ

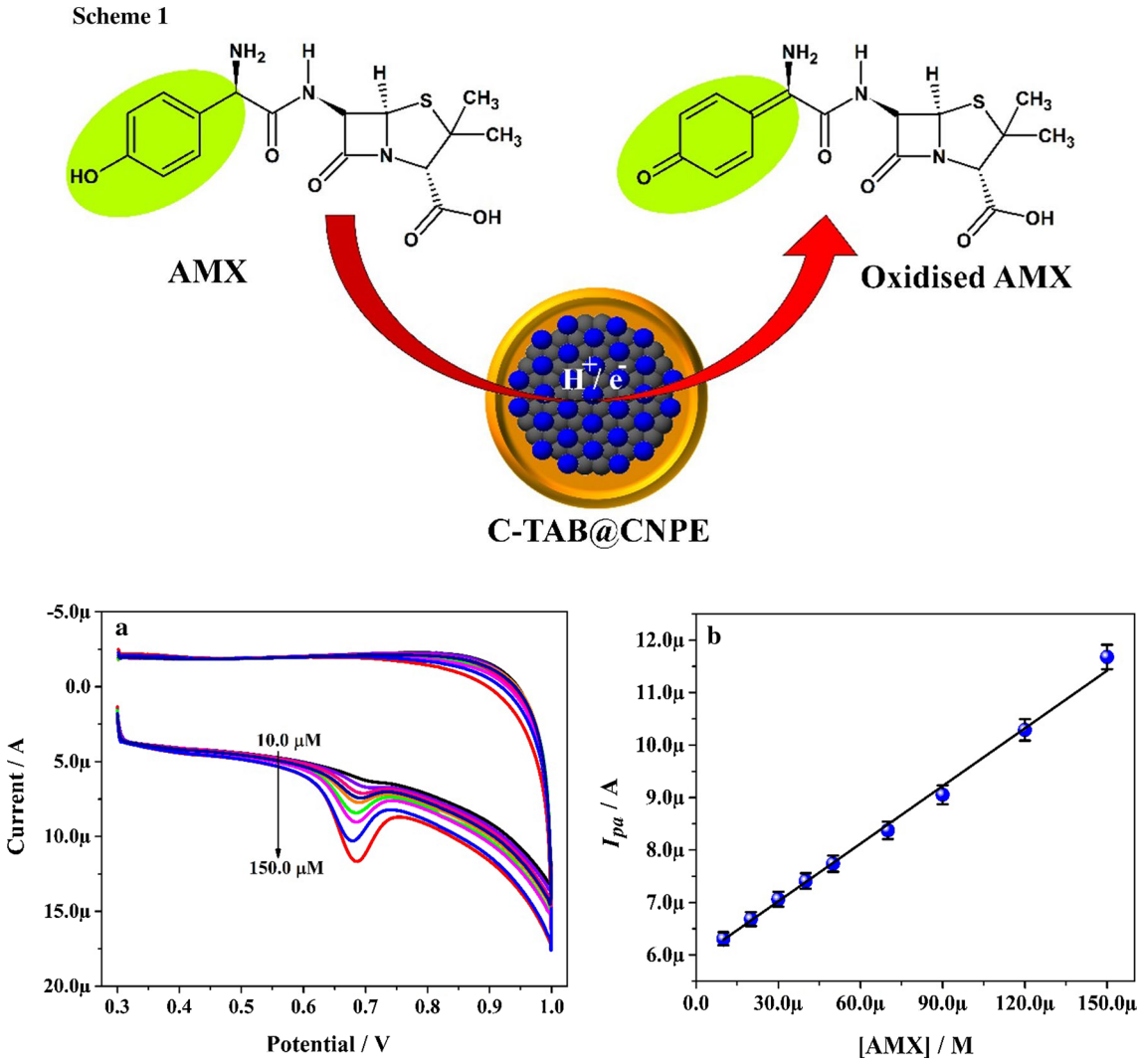

Fig. 8 **a** CVs for AMX having different concentrations from 10.0 to 150.0 µM in 0.1 M PBS (pH 6.5) on C-TAB@CNPE at the scan rate 0.1 V/s with the potential range of 0.3–1.0 V. **b** Plot of I_{pa} vs. [AMX]

Table 1 Comparison data of present AMX sensor with previously reported AMX sensors

Electrode	Linear range/µM	LOD /µM	References
Gold–palladium nanoparticles aided electrochemically reduced graphene oxide sensor	30.0–350.0	9.0	[32]
Nickel–curcumin complex modified carbon paste electrode	8.0–100.0	5.0	[33]
[*N*,*N*′-Ethylenebis(salicylideneaminato)] oxovanadium(IV) modified carbon paste electrode	18.30–35.50	16.60	[34]
Zinc oxide nanorods on gold/glass electrode	5.0–250.0	19.0	[35]
Cu/poly(*o*-toluidine) (sodium dodecyl sulfate) modified carbon paste electrode	8.0–200.0	60.0	[36]
Carbon black/dihexadecylphosphate/glassy carbon	2.0–18.80	0.120	[37]
TiO_2-CMK-3-AuNPs-Nafion@graphite electrode	2.50–133.0	0.30	[38]
Fluorescence-based sensor	12.0–72.0	12.0	[39]
C-TAB@CNPE	10.0–150.0	5.90	Present work

value of *LOD* is 5.90 µM and *LOQ* is 19.67 µM. The C-TAB@CNPE validates a lower or very nearer *LOD* for AMX than other reported AMX sensors (Table 1) [32–39]. The C-TAB@CNPE sensitivity was described using the slope of the calibration curve and the electrode surface area. The premeditated electrode sensitivity is obtained to be 1.0082 A/M/cm^2. The outcomes accomplish that, the C-TAB@CNPE displays a good electrochemical sensitivity for the inspection of AMX concentration in micromolar level.

Analysis of reproducibility, repeatability, and stability

The reproducibility, repeatability, and stability of C-TAB@CNPE were deliberated by utilizing the CV method on 0.1 mM AMX in 0.1 M PBS of pH 6.5 at 0.1 V/s scan rate. The reproducibility (Electrode is changed, n=5) and repeatability (Analyte is changed, n=5) of C-TAB@CNPE exhibits the relative standard deviation (*RSD*) of 3.59% and 2.59%, correspondingly. The stability of C-TAB@CNPE was premeditated by cycling 30 consecutive CV cycles (60 segments) and calculated using initial and final peak current values and the percentage of degradation was found to be 6.64%. Which shows that, the modified C-TAB@CNPE presents almost the equal current retort even after 30 CV cycles. This information deduces that, the C-TAB@CNPE has superior reproducibility, repeatability, and stability with first-rate detection performance during the variable time.

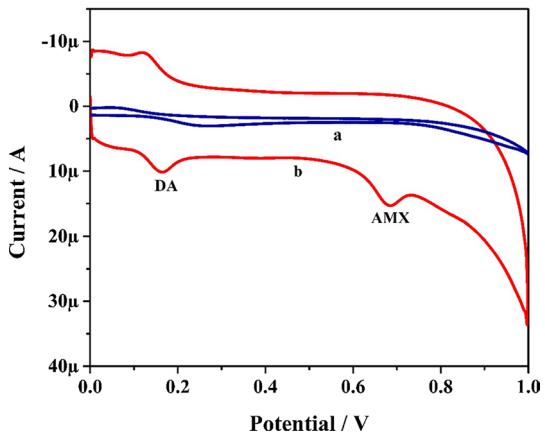

Fig. 9 CVs for 0.1 mM AMX with 1.0 mM DA in 0.1 M PBS of pH 6.5 at BCNPE (cycle *a*) and C-TAB@CNPE (cycle *b*) at the scan rate of 0.1 V/s

Selectivity of C-TAB@CNPE

The instantaneous analysis of 0.1 mM AMX with 1.0 mM DA in 0.1 M PBS of pH 6.5 at BCNPE (cycle *a*) and C-TAB@CNPE (cycle *b*) was done by operating the CV technique at the scan rate of 0.1 V/s (Fig. 9). At BCNPE, AMX and DA shows weak electrochemical response having less sensitive peak currents and high peak potentials. Nonetheless, at C-TAB@CNPE, AMX and DA moieties displays elevated electrochemical oxidation response with enhanced peak currents and reduced peak potentials. This information discloses that, the modified C-TAB@CNPE is more operative for the detection of AMX in incidence of DA with tall catalytic action and quick electron transfer than BCNPE.

Analysis of AMX in medicinal formulation

The proposed analytical outline was operated for the measurement of the quantity of AMX in the medicinal sample as a real sample. The conventional standard addition process was used for the analysis of AMX in 0.1 M PBS of 6.5 pH. The C-TAB@CNPE gives a fine recovery of 95.76–97.90% in medicinal sample (Table 2). These data detailed that, the projected electrochemical tool is very precise with elevated sensing action for AMX detection in medicinal sample.

Conclusion

In this effort, the responsive and selective C-TAB@CNPE was operated for the electrochemical analysis of AMX in presence of DA through CV method. Here, C-TAB@CNPE displays eminent electrocatalytic action for the oxidation of AMX as in case of both specific and concurrent determinations. The constructed electrochemical sensor displays higher selectivity, reproducibility, repeatability, stability, and sensitivity towards the detection of AMX. This electrochemical sensor presents very low LOD value with an outstanding linear association. Also, this projected sensor has specific applications like low-cost, easy-going preparation method and decent stability. The electrode surfaces were characterized successfully using EIS, FE-SEM, and CV approaches. The projected electrochemical tool and

Table 2 Recoveries of AMX in AMX medicinal sample

Sample used	Added/µM	Found/µM	Recovery/%
AMX medicinal sample	20	19.58	97.90
	30	28.73	95.76
	40	38.61	96.52

method give elevated sensing action for AMX detection in the medicinal sample with fine recoveries.

Experimental

CHI-6038E working model (CH Instrument-6038, USA) was used for the analysis of electro-oxidation of AMX. The three-electrode assembly was fixed in an electrochemical cell, here the saturated calomel electrode is the reference electrode, the platinum electrode is the auxiliary electrode and the C-TAB@CNPE and BCNPE are the working electrodes. The resultant oxidation potential of AMX was recorded in contradiction of the calomel electrode. EQ-610 device was operated for the preparation of different PBS pHs. FE-SEM results were documented by operating the instrument (working at the unit of kV) at DST-PURSE Lab, Mangalore University, Karnataka, India.

AMX (> 98.0% pure) was procured from Tokyo Chemical Industry Co., Ltd., India. DA (98% pure) was bought from Molychem, India. Silicone oil (98% pure), CN powder (90% pure) and potassium chloride (99.5% pure) were purchased from Nice Chemicals, India. Potassium ferrocyanide trihydrate (98.5% pure), monosodium dihydrogen phosphate (99% pure), and disodium hydrogen phosphate (99.5% pure) were procured from Himedia, India. All the used chemicals are AR graded and operated without extra purification.

Preparation of working electrodes (BCNPE and C-TAB@CNPE)

The BCNPE was achieved through the integration of silicon oil and CN powder having the weight percentage ratio of 70:30 in an agate mortar up to the uniform CN paste was accomplished. The accomplished uniform CN paste was filled in to the cavity (having 3 mm of diameter) of Teflon tube and the exterior of the tube was smoothed by scrubbing on soft paper and then the electrical reinforcement was allowed via copper lead linked to the CN paste. The C-TAB@CNPE was developed by drop-costing of 10 mm^3 C-TAB solution on the surface of obtained CNPE.

Acknowledgements N. Hareesha thankfully acknowledges the financial support to the Department of Science and Technology (DST), India for the INSPIRE Fellowship (Registration number: IF180479).

References

1. Koprowski L, Kirchmann E, Welch LE (1993) Electroanalysis 5:473
2. Garciareiriz A, Damiani P, Olivieri A (2007) Talanta 71:806
3. Uslu B, Biryol I (1999) J Pharm Biomed 20:591
4. Al-Abachi MQ, Haddi H, Al-Abachi AM (2005) Anal Chim Acta 554:184
5. Santos S, Senriques M, Duarte A, Esteves V (2007) Talanta 71:731
6. Gamba V, Dusi G (2003) Anal Chim Acta 483:69
7. Gülfen M, Canbaz Y, Özdemir A (2020) J Anal Test 4:45
8. Manjunatha JG, Kumara Swamy BE, Shreenivas MT, Mamatha GP (2012) Anal Bioanal Electrochem 4:225
9. Beitollahi H, Mazloum AM, Naeimi H, Bahram G (2009) J Solid State Electrochem 13:353
10. Manjunatha JG, Kumara Swamy BE, Deraman M, Mamatha GP (2012) Pharma Chem 4:2489
11. Sakineh EB, Beitollahi H, Somayeh T, Rahman H (2016) Int J Electrochem Sci 11:10874
12. Manjunatha JG (2016) Int J Chem Tech Res 9:136
13. Shashanka R (2018) Anal Bioanal Electrochem 10:349
14. Mohammad AK, Somayeh T, Beitollahi H, Richard AV (2020) Ind Eng Chem Res 59:4219
15. Tigari G, Manjunatha JG (2019) J Anal Test 3:331
16. Shashanka R (2021) J Iran Chem Soc 18:415
17. Pushpanjali PA, Manjunatha JG, Amrutha BM, Hareesha N (2020) Mater Res Innov 25:412
18. Beitollahi H, Raoof JB, Hosseinzadeh R (2011) Anal Sci 27:991
19. Hareesha N, Manjunatha JG, Amrutha BM, Pushpanjali PA, Charithra MM, Prinith SN (2021) J Elec Mater 50:1230
20. Somayeh T, Beitollahi H (2019) Anal Bioanal Chem Res 6:171
21. Hareesha N, Manjunatha JG (2021) Sci Rep 11:12797
22. Gururaj KJ, Kumara Swamy BE, Shashanka R, Sharma SC, Flores-Moreno R (2021) J Mol Liq 334:116348
23. Amrutha BM, Manjunatha JG, Aarti SB, Nagarajappa H (2021) J Sci: Adv Mater Devices 6:415
24. Shashanka R, Kumara Swamy BE (2020) Phys Chem Res 8:1
25. Pushpanjali PA, Manjunatha JG, Nagarajappa H, D'Souza ES, Charithra MM, Prinith NS (2021) Surf Interfaces 24:101154
26. Shashanka R, Taslimi P, Karaoglanli AC, Uzun O, Alp E, Jayaprakash GK (2021) Arab J Chem 14:103180
27. Hareesha N, Manjunatha JG (2020) J Sci: Adv Mater Devices 5:502
28. Manjunatha JG, Swamy BEK, Gilbert O, Mamatha GP, Sherigara BS (2010) Int J Electrochem Sci 5:682
29. Hareesha N, Manjunatha JG, Amrutha BM, Sreeharsha N, BasheeruddinAsdaq SM, Khalid Anwer Md (2021) Colloids Surf A Physicochem Eng Asp 626:127042
30. Pham TH, Mai T, Nguyen HA, Chu TT, Vu T, Le QH (2021) J Anal Methods Chem 2021:8823452
31. Manjunatha JG (2020) Chem Data Coll 25:100331
32. Kumar N, Rosy RN, Goyal RN (2017) Sens Actuators B Chem 243:658
33. Ojani R, Raoof JB, Zamani S (2012) Bioelectrochemistry 85:44
34. Bergamini MF, Teixeria MFS, Dockal ER, Bocchi N, Cavalheiro ETG (2006) J Electrochem Soc 153:E94
35. Hatamie A, Echresh A, Zargar B, Nur O, Willander M (2015) Electrochim Acta 174:1261
36. Norouzi B, Mirkazemi T (2016) Russ J Electrochem 52:37
37. Deroco PB, Rocha-Filho RC, Fatibello-Filho O (2018) Talanta 179:115
38. Pollap A, Knihnicki P, Kuśtrowski P, Kozak J, Gołda-Cępa M, Kotarba A, Kochana J (2018) Electroanalysis 30:2386
39. Pawar SP, Walekar LS, Gunjal DB, Dalavi DK, Gore AH, Anbhule P, Patil S, Kolekar G (2017) Luminescence 32:918